Nuclear Instruments and Methods in Physics Research B43 (1989) 471–483
North-Holland, Amsterdam

MECHANISMS OF ION NEUTRALIZATION AT SURFACES IN FAST COLLISIONS

U. THUMM and J.S. BRIGGS

Fakultät für Physik, Albert-Ludwigs-Universität, Hermann-Herder-Str. 3, D-7800 Freiburg, FRG

Received 13 April 1989 and in revised form 1 June 1989

We present an analysis of higher-order processes in the capture of an electron from a surface by grazing-incidence impact of an ion moving at velocities greater than the Fermi velocity. In first order the capture probability is known to decrease very rapidly with increasing projectile velocity. The dominant process is shown to be of second order, in which surface electrons are scattered by the projectile ion and then recoil off the lattice atomic cores, to emerge from the surface with the same velocity as the ion. This Thomas-scattering process is well-known in the study of ion–gas collisions. In the case of a solid target it shows many formal similarities to the process of LEED.

1. Introduction

The theory of the capture of electrons from atoms by fast incident ions has developed significantly in the past twenty years (see for example the reviews by Belkić et al. [1], Shakeshaft and Spruch [2] and Briggs [3]). The regions of low and high velocities are distinguished by whether the initial relative velocity in the centre-of-mass frame is smaller or greater than the typical orbital velocities of the electrons to be captured. At low velocity, capture probabilities are calculated by assuming that in zeroth order the electrons move almost adiabatically in the field of both nuclei and a "quasi-molecular" collision complex is formed. At high velocity the target electrons must acquire the translational velocity and kinetic energy of the projectile in order to be captured. This kinematic effect manifests itself in the theory by the appearance of Galilei transformation or "translation" factors in transition matrix elements. Beginning with the classical work of Thomas [4] these effects have been studied in detail [2,5–7]. It has been shown clearly that the target electron may acquire the necessary translational momentum either by virtue of its binding in the initial or final state (a three-body collision) or by a sequence of two two-body collisions (Thomas mechanism). In a Born expansion of the capture transition matrix element, the three-body mechanism occurs in the first and higher terms whereas the Thomas double-binary collision term occurs only in the second and higher terms of the Born series. At high velocities, since the probability of high momentum components in the bound states decreases rapidly, it is the double-binary collision component of the second Born term that provides the dominant contribution to the capture cross-section. Although providing the dominant term it has also become clear that, because of the infinite-range Coulomb potential, the second Born term alone is not adequate to describe capture and an infinite-order scattering approximation is necessary at high velocity. Several such theories have been advanced over the years [1,8–13].

There is increasing interest in the capture of electrons from solid surfaces by impinging ions [14,15]. At low ion velocities (now measured with respect to electron velocities at the Fermi level) the situation is similar to the atomic case in that electrons tunnel or are shared between the potential wells of the solid and projectile. In addition, collision velocities may be sufficiently low that translation (Galilei transformation) effects between the stationary solid and the projectile are negligible. Rather it is the occurrence of resonances between dynamically-shifted projectile and target states that decides the capture probability. At high velocity, as in the atomic target case, the situation changes dramatically in that it is the matching of initial and final states in momentum space, represented by a Galilei shift of the Fermi momentum distribution with respect to the moving projectile, that is decisive in determining capture. This much has been recognized [14,15]. However, although first-order theories [16–20] and coupled-state higher-order theories [21] have been advanced, the surface analogue of the Thomas double-binary mechanism has not been considered explicitly. It is our purpose in this paper to remedy this situation by considering the higher order terms known to be of importance for atomic targets.

That higher-order processes are significant in capture from surfaces can be readily seen by considering an idealized situation. Were the target electrons to be considered as truly free, i.e. in plane-wave states, then a single interaction between projectile and electron (first

Born approximation) could not lead to capture, i.e. two free particles cannot collide to form a bound state. However a double-binary collision could. In the latter case the electron is first struck by the projectile and acquires its speed (but not its vector velocity!). This fast electron then recoils off the solid, changing direction so that it emerges from the surface with the same velocity vector as the projectile and is readily captured.

Since the target electrons in their initial state are not truly free, there is of course a contribution to capture from the first-order Born mechanism. However, as we will show, this contribution is proportional to the probability of target-electron velocity components of the same order of magnitude as those of the incident ion. Hence for an ion at grazing incidence, traveling essentially parallel to an ideal surface, it is the Fermi momentum components parallel to the surface that are decisive. Therefore, as appreciated by Andrä and coworkers [14,15], the capture probability due to this mechanism would be expected to decrease rapidly for parallel velocities greater than the Fermi velocity. One should note however that this only remains true so long as the perpendicular velocity is so small that the incident ion does not penetrate the inner shells of the surface atoms. Such inner-shell electrons possess high momentum components and can be captured in close collisions.

It is perhaps interesting to note that our proposed higher-order collision mechanism for surface capture bears much resemblance to the process of low-energy electron diffraction (LEED) and this analogy will emerge directly from the theory presented below. In LEED a beam of electrons impinges on the solid surface and is scattered coherently by the surface layers considered as a spatially-distributed array of scattering centres [22–24]. In our mechanism the Coulomb field of the impinging ion sets the surface electrons themselves in motion. Thereafter, however, their scattering by the solid surface is identical to the LEED process. In the case of capture, the capture probability is obtained by folding the momentum distribution of electrons emerging from the surface with the momentum distribution of bound states on the moving projectile. It is this folding procedure and, in addition, the incoherent sum over initial states, which washes out the coherent diffraction effects observed in LEED spectra.

The plan of the paper is as follows. In section 2 the formal theory of scattering of grazing incidence ion beams leading to surface-electron capture is presented in which the ion beam is treated classically. In section 2.1 systematics of the exact transition matrix element are discussed and related to its first and second order approximation. In section 2.2 the transition amplitude in the first Born approximation is evaluated. The dependence on the projectile incidence angle and velocity is discussed and numerical results are given for different systems. In section 2.3 the second order contribution is considered. The new double binary mechanism is identified and related to the Thomas process and the process of electron diffraction. Section 3 contains our conclusions.

Atomic units with e (electron charge), m (electron mass) and $\hbar$ equal to unity are used unless otherwise stated.

2. Theory of electron capture

2.1. The impulse approximation and LEED

In formulating the amplitude for electron capture it will be assumed that the incident ion moves on a prescribed classical trajectory $\boldsymbol{R}(t)$ with respect to an arbitrary origin located in the surface. The exact transition amplitude for a single electron, initially bound in the solid, to transfer to a bound state of the projectile is given by [25]

$$f = -\mathrm{i}\int_{-\infty}^{\infty} \langle \Psi_{\mathrm{f}}^{-}(t) | V_{\mathrm{P}}(t) | \Phi_{\mathrm{i}}(t) \rangle \, \mathrm{d}t. \tag{1}$$

Here $\Phi_{\mathrm{i}}(t) = \phi_{\mathrm{i}}(\boldsymbol{r}) \exp(-\mathrm{i}\epsilon_{\mathrm{i}} t)$ is the initial wavefunction of the electron with co-ordinate $\boldsymbol{r}$ with respect to the fixed origin and binding energy ϵ_{i}. The potential $V_{\mathrm{P}}(t) = -Z_{\mathrm{P}}/|\boldsymbol{r} - \boldsymbol{R}(t)|$ is the time-dependent Coulomb potential of the projectile ion and $\Psi_{\mathrm{f}}^{-}(t)$ is an exact scattering state of the captured electron, represented formally by

$$\Psi_{\mathrm{f}}^{-}(t) = \Phi_{\mathrm{f}}(t) - \mathrm{i}\int_{t}^{\infty} U(t, t') V_{\mathrm{T}} \Phi_{\mathrm{f}}(t') \, \mathrm{d}t' \tag{2}$$

That is, $\Psi_{\mathrm{f}}^{-}(t)$ is the exact scattering state propagating backwards in time from the final electronic bound state of the projectile

$$\Phi_{\mathrm{f}}(t) = \phi_{\mathrm{f}}(\boldsymbol{r}') \exp\{-\mathrm{i}\epsilon_{\mathrm{f}} t - \mathrm{i}\tfrac{1}{2} v^2 t + \mathrm{i}\boldsymbol{v}\cdot\boldsymbol{r}\}, \tag{3}$$

where $\boldsymbol{r}' \equiv \boldsymbol{r} - \boldsymbol{R}(t)$, ϵ_{f} is the binding energy and $\boldsymbol{v} = \dot{\boldsymbol{R}}$ is the instantaneous velocity of the projectile. The additional exponential factors in (3) describe the translational momentum and kinetic energy of an electron moving bound to the projectile ion. The potential V_{T} represents the (time-independent) potential of the solid target and this will be specified in more detail later. The operator $U(t, t')$ is the full time-development operator of an electron moving under the influence of both potentials $V_{\mathrm{P}}(t)$ and V_{T}. This operator satisfies the integral equation

$$U(t, t') = U_{\mathrm{T}}(t, t') - \mathrm{i}\int_{t'}^{t} U_{\mathrm{T}}(t, t'') V_{\mathrm{P}}(t'') U(t'', t') \, \mathrm{d}t'', \tag{4}$$

where

$$U_{\mathrm{T}}(t, t') = \exp\{-\mathrm{i}H_{\mathrm{T}}(t - t')\} \tag{5}$$

with $H_T = K + V_T$, where K is the electron kinetic energy operator. The expression (2) is exact within the one-electron classical-trajectory approximation. The key additional approximation, which exposes the connection to the LEED phenomenon, is to assume that during the collision the dominant scattering mechanism is that of the electron with the cores of the heavy atoms comprising the solid. This corresponds to the neglect of the second term on the RHS of (4) i.e. to the replacement of the full propagator $U(t, t')$ by the target propagator $U_T(t, t')$. This replacement in (2) allows the capture amplitude (1) to be written in the form

$$f = -i\int_{-\infty}^{\infty} dt \langle \Phi_f(t) | V_P(t) | \Phi_i(t) \rangle + \int_{-\infty}^{\infty} dt \times \int_{t}^{\infty} dt' \langle \Phi_f(t') | V_T U_T(t', t) V_P(t) | \Phi_i(t) \rangle. \quad (6)$$

The first term is the first Born approximation and the second represents a single scattering off the projectile followed by infinite-order scattering off the solid target. In the case of an atomic target, this approximation is well-known under the name of impulse approximation (IA) or strong potential Born approximation (SPB). Since the target potential is considered dominant in the scattering process, the IA is only likely to be valid when the collision is fast (compared with the Fermi velocity) and the projectile charge is low. It will certainly not be valid to describe capture by highly-stripped slow ions.

The connection to the scattering amplitude for low-energy electron diffraction is exposed by writing (6) in the form

$$f = -i\int_{-\infty}^{\infty} dt \Big\langle \langle \Phi_f(t) | + i\int_{t}^{\infty} dt' \langle \Phi_f(t') | V_T U_T(t', t) \Big\rangle V_P(t) | \Phi_i(t) \rangle \quad (7)$$

and introducing a complete set of plane-wave states (eigenstates of the electron kinetic energy operator K) at fixed time, i.e.

$$f = -i\int_{-\infty}^{\infty} dt \int d\boldsymbol{q}'\, d\boldsymbol{q} \Big\langle \langle \Phi_f(t) | \boldsymbol{q}(t) \rangle \langle \boldsymbol{q}(t) | + i\int_{t}^{\infty} dt' \langle \Phi_f(t') | \boldsymbol{q}(t') \rangle \langle \boldsymbol{q}(t') | V_T U_T(t', t) \Big\rangle \times | \boldsymbol{q}'(t) \rangle \langle \boldsymbol{q}'(t) | V_P(t) | \Phi_i(t) \rangle. \quad (8)$$

The scattered wave

$$| \chi_{\boldsymbol{q}}(t) \rangle = | \boldsymbol{q}(t) \rangle - i\int_{t}^{\infty} dt' U_T(t, t') V_T | \boldsymbol{q}(t') \rangle \quad (9)$$

embedded in (8) is the scattered wave which would be produced by a plane-wave beam of free electrons impinging on the solid surface, as in a LEED experiment. Hence the physical interpretation of the capture process described by (8) is obtained by reading the matrix element from right to left. An initial stationary distribution of target electrons, represented by the initial target wave function Φ_i, is scattered into a distribution of momentum states $| \boldsymbol{q}' \rangle$. Each component $\boldsymbol{q}'$ scatters off the target an infinite number of times to emerge in the scattered wave $\chi_{\boldsymbol{q}}(t)$. The final capture amplitude is obtained by folding the distribution of electrons emerging from the scattering (LEED) process with the momentum space wave function $\langle \Phi_f(t') | \boldsymbol{q}(t') \rangle$ of the final projectile bound state at each instant in time.

If no intermediate scattering occurs, i.e. the potential V_T in (8) is switched off, one has the first Born term

$$f_{B1} = -i\int_{-\infty}^{\infty} dt \times \int d\boldsymbol{q} \langle \Phi_f(t) | \boldsymbol{q}(t) \rangle \langle \boldsymbol{q}(t) | V_P(t) | \Phi_i(t) \rangle = -i\int_{-\infty}^{\infty} dt \langle \Phi_f(t) | V_P(t) | \Phi_i(t) \rangle, \quad (10)$$

since $\langle \boldsymbol{q} | \boldsymbol{q}' \rangle = \delta^{(3)}(\boldsymbol{q} - \boldsymbol{q}')$.

In order to isolate the different physical nature of the first Born (10) and impulse (7) approximations to the capture amplitude and their different dependence on the experimental parameters, the two will be discussed separately. In fact the major dynamical features of multiple scattering (IA) will be discussed by considering only a single scattering off the lattice atoms i.e. in second Born approximation.

2.2. The first Born approximation

In the first Born approximation (10), capture is considered to take place by a single interaction between the target electron and the projectile nucleus. The electron transfers between undistorted initial and final states, whose energy is constant. Although such a description is only valid, if at all, at high velocities this first order term is the basic form of the interaction considered in previous perturbative theories [18–20] of electron capture not involving Auger or auto-ionization processes. However, at lower velocity account has been taken [21] of the important energy shifts of the atomic levels which take place when an ion approaches a surfaces. The only energy shifts arising in the first order Born approximation are those due to the electron translation factors. In this paper attention will be concentrated on these kinematic effects in fast collisions.

In order to perform the time integral in (10) it is necessary to specify the ion trajectory $\boldsymbol{R}(t)$. As we wish to emphasize the physical effects of the interaction, the most suitable form for our purpose is the "broken line" trajectory depicted in fig. 1. Such a trajectory allows the time integrals to be performed analytically but is nevertheless a sufficiently realistic approximation to the true trajectory that no fundamentally new effects would be

expected to arise from the use of a more exact description of the classical motion. For a co-ordinate system with the x–y plane in the surface and the positive z-axis along the surface normal towards the vacuum, the broken line trajectory is parametrized by

$$\boldsymbol{R}(t) = b\hat{\boldsymbol{e}}_z + \boldsymbol{v}_\pm t, \tag{11}$$

$$\boldsymbol{v}(t) = v_\parallel \hat{\boldsymbol{e}}_x \pm v_\perp \hat{\boldsymbol{e}}_z \equiv \boldsymbol{v}_\pm, \tag{12}$$

where + (−) correspond to $t > 0$ ($t < 0$), i.e. to the outgoing (incoming) part of the trajectory, respectively. The projectile velocity parallel to the surface is denoted by $\boldsymbol{v}_\parallel = (v_\parallel, 0, 0)$. The velocity perpendicular to the surface for the outgoing (incoming) path is $v_\perp$ ($-v_\perp$), respectively. The distance b depends on $v_\perp$ and is treated as a parameter of the theory. For the special case $v_\perp = 0$, eq. (11) gives a straight line trajectory with impact parameter b. The vector $\boldsymbol{b} = (0, 0, b)$ is used to simplify notation.

With Fourier transforms and plane waves introduced according to

$$\tilde{\phi}(\boldsymbol{q}) = (2\pi)^{-3/2} \int \mathrm{d}\boldsymbol{r} \exp\{-\mathrm{i}\boldsymbol{q}\cdot\boldsymbol{r}\}\,\phi(\boldsymbol{r}) \tag{13}$$

$$\langle \boldsymbol{r} \,|\, \boldsymbol{q}(t)\rangle = (2\pi)^{-3/2} \exp\{\mathrm{i}\boldsymbol{q}\cdot\boldsymbol{r} - \mathrm{i}\tfrac{1}{2}q^2 t\}, \tag{14}$$

the momentum distribution of the Galilei-shifted final state in (10) is

$$\begin{aligned}\langle \boldsymbol{q}(t) \,|\, \Phi_f(t)\rangle &= \tilde{\phi}_f(\boldsymbol{q} - \boldsymbol{v}(t)) \exp\{-\mathrm{i}(\boldsymbol{q} - \boldsymbol{v}(t))\cdot\boldsymbol{R}(t) \\ &\quad - \mathrm{i}(\epsilon_f + \tfrac{1}{2}v^2 - \tfrac{1}{2}q^2)t\},\end{aligned} \tag{15}$$

where $\boldsymbol{q}$ is defined with respect to the solid frame of reference. $\tilde{\phi}_f$ is the final projectile state momentum wavefunction.

Introducing a second complete set of plane waves between $V_P(t)$ and $|\Phi_i(t)\rangle$ and using (15) we obtain from (10)

$$\begin{aligned} f_{B1} &= -ri\int_{-\infty}^{\infty} \mathrm{d}t \int \mathrm{d}\boldsymbol{q}\, [\Phi_f(t) \,|\, \boldsymbol{q}(t)\rangle \\ &\quad \times \langle \boldsymbol{q}(t) \,|\, V_P(t) \,|\, \boldsymbol{p}(t)\rangle \langle \boldsymbol{p}(t) \,|\, \Phi_i(t)\rangle \\ &= -\mathrm{i}(2\pi)^{-3/2} \int \mathrm{d}\boldsymbol{q}\, \mathrm{d}\boldsymbol{p}\, \tilde{\phi}_f^*(\boldsymbol{q} - \boldsymbol{v}(t)) \\ &\quad \times \exp\{\mathrm{i}(\boldsymbol{p} - \boldsymbol{v}(t))\cdot\boldsymbol{b}\}\, \tilde{V}_P(\boldsymbol{q} - \boldsymbol{p})\, \tilde{\phi}_i(\boldsymbol{p}) \\ &\quad \times \int_{-\infty}^{\infty} \mathrm{d}t \exp\{\mathrm{i}(\boldsymbol{p}\cdot\boldsymbol{v}(t) + \Delta\epsilon - \tfrac{1}{2}v^2)t\}, \end{aligned} \tag{16}$$

where

$$\Delta\epsilon \equiv \epsilon_f - \epsilon_i \tag{17}$$

and

$$\tilde{V}_P(\boldsymbol{q} - \boldsymbol{p}) = \sqrt{\frac{2}{\pi}}\, \frac{Z_P}{|\boldsymbol{q} - \boldsymbol{p}|^2} \tag{18}$$

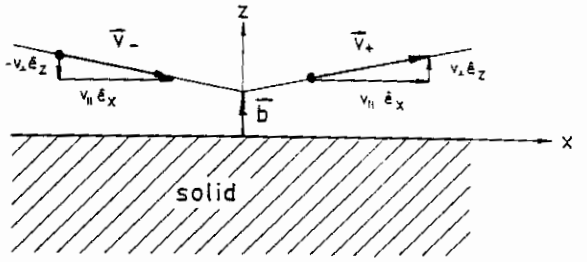

Fig. 1. Coordinate system and broken straight line trajectory, for the special case $b > 0$, where the projectile nucleus does not intersect the electronic surface (identical to the $z = 0$ plane). The projectile velocity on the incoming and outgoing straight line segment is v_- and v_+, respectively.

is the Fourier transform of the projectile Coulomb potential.

For a straight line trajectory parallel to the surface ($v_\perp = 0$, $v = v_\parallel$) the time integral in (16) is proportional to a δ-function incorporating energy conservation. Then the transition amplitude becomes identical to the expression well known from the semiclassical description of gas-phase collisions [26,27]

$$\begin{aligned} f_{B1} &= -\mathrm{i}(2\pi)^{-1/2} \int \mathrm{d}\boldsymbol{q}\, \mathrm{d}\boldsymbol{p}\, \tilde{\phi}_f^*(\boldsymbol{q} - \boldsymbol{v}) \\ &\quad \times \exp\{\mathrm{i}\boldsymbol{p}\cdot\boldsymbol{b}\}\, \tilde{V}_p(\boldsymbol{q} - \boldsymbol{p})\, \tilde{\phi}_i(\boldsymbol{p}) \\ &\quad \times \delta(p_x v + \Delta\epsilon - \tfrac{1}{2}v^2). \end{aligned} \tag{19}$$

The δ function expresses the condition

$$p_x = \tfrac{1}{2}v - \frac{\Delta\epsilon}{v}, \tag{20}$$

such that for $v \gg \Delta\epsilon$ only momentum components of the initial state with $p_x \approx \frac{1}{2}v$ contribute to (19). Since the initial state momentum distribution is in general concentrated in a finite region of momentum space, the first order scattering amplitude decreases rapidly for large v. We shall see below that this is also true for a broken line trajectory in connection with jellium initial state wavefunctions.

For a broken line trajectory we split the time integral in (16) and consider the contribution of the outgoing and incoming trajectory, f_{B1}^- and f_{B1}^+, separately,

$$f_{B1} = f_{B1}^- + f_{B1}^+ \tag{21}$$

$$\begin{aligned} f_{B1}^\pm &= \pm(2\pi)^{-3/2} \lim_{\eta\to 0} \int \mathrm{d}\boldsymbol{q}\, \mathrm{d}\boldsymbol{p}\, \tilde{\phi}_f^*(\boldsymbol{q} - \boldsymbol{v}_\pm) \\ &\quad \times \tilde{V}_P(\boldsymbol{q} - \boldsymbol{p})\, \tilde{\phi}_i(\boldsymbol{p}) \\ &\quad \times [\boldsymbol{p}\cdot\boldsymbol{v}_\pm + \Delta\epsilon - \tfrac{1}{2}v^2 \pm \mathrm{i}\eta]^{-1} \\ &\quad \times \exp\{\mathrm{i}(\boldsymbol{p} - \boldsymbol{v}_\pm)\cdot\boldsymbol{b}\}, \end{aligned} \tag{22}$$

where η is a positive infinitesimal.

The q-integral in (22) can be evaluated in closed form for an arbitrary hydrogenic final state [28]. For a hydrogenic ground state it reads

$$\int \mathrm{d}\,\boldsymbol{q}\;\tilde{\phi}_{1s}^{*}(\boldsymbol{q}-\boldsymbol{v}_{\pm})\tilde{V}_{P}(\boldsymbol{q}-\boldsymbol{p}) = -4\sqrt{\pi}\,Z_P^{5/2}\frac{1}{|\boldsymbol{p}-\boldsymbol{v}_{\pm}|^2+Z_P^2}. \tag{23}$$

We now specify the initial state, assuming that capture takes place out of a delocalized band state. In the jellium approximation the band electrons are considered as essentially free within the metal volume V, but bound to the metal half-space by a potential step

$$V_0 = \epsilon_F + W \tag{24}$$

situated at the surface. For zero temperature the band states are occupied up to the Fermi level ϵ_F. The minimum energy necessary to ionize a target electron is given by the work function W. In momentum space all occupied states ϕ_k, labeled by the momentum $\boldsymbol{k}$, lie in the Fermi sphere of radius $k_F = \sqrt{2\epsilon_F}$ with the constant free-electron density of states

$$\rho = V/4\pi^3, \tag{25}$$

where a factor 2 for the spin degrees of freedom is included. In co-ordinate space the jellium wavefunctions are given by

$$\phi_k(\boldsymbol{r}) = \frac{1}{\sqrt{V}}\exp\{\mathrm{i}\boldsymbol{k}_{\parallel}\cdot\boldsymbol{r}_{\parallel}\} \times\begin{cases}\exp\{\mathrm{i}k_z z\}+R\exp\{-\mathrm{i}k_z z\} & z<0\\ T\exp\{-\gamma z\} & z>0\end{cases} \tag{26}$$

with

$$\gamma \equiv \sqrt{2V_0 - k_z^2} \tag{27}$$

and the reflection- and transmission coefficients

$$R \equiv \frac{k_z-\mathrm{i}\gamma}{k_z+\mathrm{i}\gamma}, \qquad T \equiv \frac{2k_z}{k_z+\mathrm{i}\gamma}. \tag{28}$$

The corresponding momentum space wave functions are

$$\tilde{\phi}_k(\boldsymbol{p}) = \delta^{(2)}(\boldsymbol{k}_{\parallel}-\boldsymbol{p}_{\parallel})\,\tilde{u}_{k_z}(p_z), \tag{29}$$

with

$$\tilde{u}_{k_z}(p_z) = \sqrt{\frac{2\pi}{V}}\,\mathrm{i}\left\{\frac{1}{p_z-k_z+\mathrm{i}\delta}+\frac{R}{p_z+k_z+\mathrm{i}\delta}-\frac{T}{p_z-\mathrm{i}\gamma}\right\}, \tag{30}$$

where the positive, infinitesimal convergence factor δ is used for the part of the wavefunction inside the solid to account for the infinite extension of the metal along the negative z-axis.

With (23) and (29) the transition amplitude (22) for capture into a hydrogenic ground state becomes

$$f_{B1}^{\pm} = \mp\frac{\sqrt{2}}{\pi}Z_P^{5/2}\exp\{-\mathrm{i}v_{\pm}\cdot b\}\int \mathrm{d}p_z\,\exp\{\mathrm{i}p_z b\} \times\left[\boldsymbol{k}_{\parallel}\cdot\boldsymbol{v}_{\parallel}\pm p_z v_{\perp}+\Delta\epsilon-\tfrac{1}{2}v^2\pm\mathrm{i}\eta\right]^{-1} \times\left[(p_z\mp v_{\perp})^2+F^2\right]^{-1}\tilde{u}_{k_z}(p_z), \tag{31}$$

where

$$F^2 \equiv k_{\parallel}'^2 + Z_P^2, \qquad \boldsymbol{k}_{\parallel}' \equiv \boldsymbol{k}_{\parallel}-\boldsymbol{v}_{\parallel}. \tag{32}$$

For $b>0$, i.e. if the projectile nucleus does not penetrate the electronic surface defined by the jellium edge (the $z=0$-plane), the remaining integral over p_z is evaluated by closing the contour in the upper complex half-plane and calculating the residues of the single poles at $p_z = \pm v_{\perp}+\mathrm{i}F$ and $p_z = \mathrm{i}\gamma$. The result can be summarized in the form,

$$f_{B1}^{\pm} = -2\sqrt{2}\,\mathrm{i}Z_P^{5/2}\left\{\mathrm{Res}(\pm v_{\perp}+\mathrm{i}F)+\mathrm{Res}(\mathrm{i}\gamma)^{\pm}\right\}, \tag{33}$$

where

$$\mathrm{Res}(\pm v_{\perp}+\mathrm{i}F) \equiv \frac{1}{\mathrm{i}Fv_{\perp}\pm\alpha}\frac{1}{2\mathrm{i}F}\tilde{u}_{k_z}(\mathrm{i}F\pm v_{\perp})\exp\{-Fb\} \tag{34}$$

$$\mathrm{Res}(\mathrm{i}\gamma)^{\pm} \equiv -\sqrt{\frac{2\pi}{V}}\,\mathrm{i}T\frac{1}{(\mp v_{\perp}+\mathrm{i}\gamma)v_{\perp}\pm\alpha} \times\frac{1}{(\mp v_{\perp}+\mathrm{i}\gamma)^2+F^2} \times\exp\{\mp\mathrm{i}v_{\perp}b-\gamma b\} \tag{35}$$

and

$$\alpha \equiv \Delta\epsilon+\boldsymbol{k}_{\parallel}\cdot\boldsymbol{v}_{\parallel}-\tfrac{1}{2}v^2. \tag{36}$$

Similarly, for $b<0$, i.e. if the projectile trajectory intersects the electronic surface twice, contour integration results in calculating the residues of the single poles at $p_z = k_z-\mathrm{i}\delta$, $p_z = -k_z-\mathrm{i}\delta$, $p_z = \pm v_{\perp}-\mathrm{i}F$ and $p_z = \pm v_{\perp}\mp\alpha/v_{\perp}-\mathrm{i}\eta$ in the lower half plane. With the free particle dispersion relation

$$\epsilon_i = -V_0+\tfrac{1}{2}k^2 \tag{37}$$

α can be rewritten as

$$\alpha = \epsilon_f+V_0-\tfrac{1}{2}k_{\parallel}'^2-\tfrac{1}{2}k_z^2-\tfrac{1}{2}v_{\perp}^2. \tag{38}$$

Therefore the transition amplitude appears as a function of the length of the shifted parallel momentum $k_{\parallel}'$ (32) of the target electron and k_z, i.e. as a function of two parameters only instead of the three components of $\boldsymbol{k}$ which characterize the initial wave function. The first order transition probability

$$P_{B1} = \int_{k\le k_F}\mathrm{d}\boldsymbol{k}\;\rho\,|f_{B1}(\boldsymbol{k})|^2 \tag{39}$$

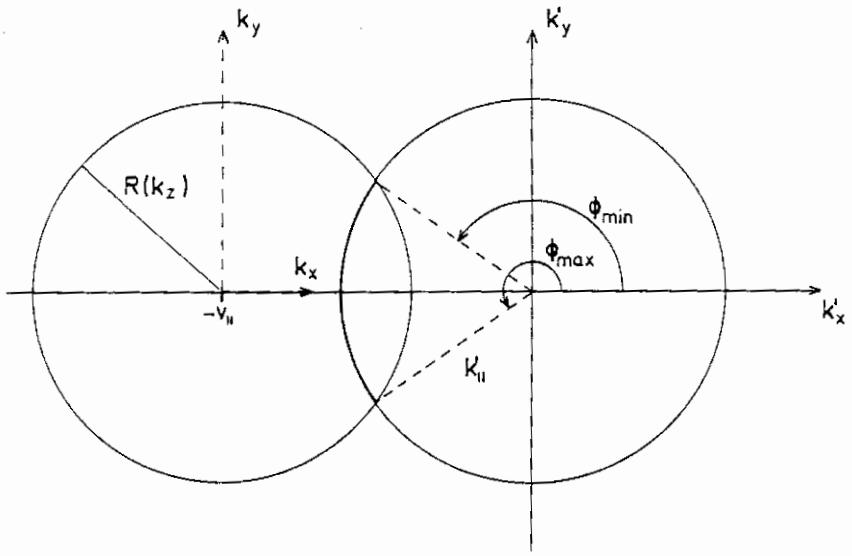

Fig. 2. Projection of the $v_\parallel$-shifted and unshifted Fermi sphere on the surface ($k_x - k_y$ plane). The angles $\phi_{min}(k'_\parallel)$ and $\phi_{max}(k'_\parallel)$ define the range of the k'_ϕ integration after transformation to the shifted parallel momentum $k'_\parallel$ [see eqs. (39) to (41)].

is then obtained by two additional integrations, i.e.

$$P_{B1} = \rho \int_{-k_F}^{k_F} \int_{k'_\parallel \le R(k_z)} dk'_\parallel \, k'_\parallel \left| f_{B1}(k_z, k'_\parallel) \right|^2 \times \left[\phi_{max}(k'_\parallel) - \phi_{min}(k'_\parallel) \right], \quad (40)$$

where the functions ϕ_{max} and ϕ_{min} are defined by fig. 2, and

$$R(k_z) \equiv \sqrt{k_F^2 - k_z^2} + v_\parallel. \quad (41)$$

The two integrals over the band momenta must be performed numerically.

It is instructive to consider the limiting case of a straight line trajectory in (31). For $v_\perp = 0$ the two contributions $f_{B1}^{\pm}$ contain the factor $\pm(\alpha \pm i\eta)^{-1}$ respectively. However, since

$$\frac{\pm 1}{\alpha \pm i\eta} = \frac{\pm P}{\alpha} - i\pi\delta(\alpha), \quad (42)$$

the principal part contributions cancel in the sum (21). Hence, in this limit, the amplitude f_{B1} contains a factor $\delta(a)$, which appears outside the p_z integral. It follows that only those metal electrons with momenta such that $\alpha = 0$ can be captured. This condition is the surface analogue of that arising in the straight line trajectory in gas-phase collisions (eq. (20)). For jellium initial states, the condition is explicitly

$$k_x = \tfrac{1}{2}v - \frac{\Delta\epsilon(k'_\parallel, k_z)}{v}. \quad (43)$$

With (37), the condition (43) can be written as

$$\tfrac{1}{2}k^2 = \epsilon_f + V_0 + k_\parallel v - \tfrac{1}{2}v^2. \quad (44)$$

Since k has an upper limit k_F, one sees that as v increases there comes a velocity at which (44) cannot be satisfied. Therefore the first Born, parallel-trajectory amplitude suddenly decreases to zero above a certain projectile velocity v.

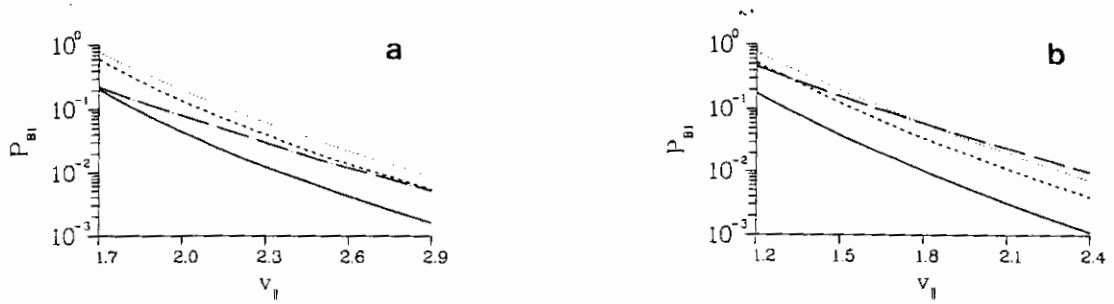

Fig. 3. (a) Neutralization probability due to K-shell capture for protons colliding with an aluminium surface. Result in first order [eq. (40)] for the perpendicular velocities: ——— $v_\perp = 0.1$; - - - - - - $= 0.2$; · · · · · · $= 0.3$; · – · – · $= 0.6$ (in a.u.). (b) As (a) but for a tungsten surface.

For grazing incidence collisions the first order amplitude still decreases rapidly for large $v_\parallel$. However, the decrease is slower with increasing perpendicular velocity $v_\perp$. The reason for this is again best seen in (31). For $v_\perp > 0$ the first denominator does not lead to the restriction (43), since the principal parts for $\pm\eta$ do not cancel. Rather, the principal part contribution is folded with the z-component of the initial state momentum distribution. Since jellium wave functions decay exponentially outside the solid, the momentum distribution $\tilde{u}_{k_z}(p_z)$ contains contributions from all p_z. Capture therefore becomes possible even if (43) does not hold, due to the pick up of the appropriate perpendicular momentum p_z. The transmitted part of $\tilde{u}_{kz}$ [third term in (30)] is concentrated at $p_z = 0$. From the structure of (31) one sees that the small p_z components are increasingly important in deciding the capture amplitude as $v_\perp$ increases.

In fig. 3 the velocity dependent behaviour of the first order neutralization amplitude is shown for the cases of aluminium and tungsten surfaces. In both examples capture into the ground state is assumed. Due to the relative broad conduction band of aluminium, the hydrogen ground state is in resonance with the band as long as the kinematic shift does not 'move' the discrete level out of resonance (compare fig. 4a). Therefore at constant and small $v_\parallel$ the discrete level is in or close to resonance and the transition probability decreases at relatively large $v_\perp$ as $v_\perp$ increases in agreement with a simple collision time consideration (fig. 3a). At constant and large $v_\parallel$ the discrete level is far out of resonance and the $v_\perp$-dependence of P_{B1} changes qualitatively. Now capture only becomes possible through the higher momentum components of $\tilde{u}_{k_z}$, as explained above, and the probability decays faster as a function of $v_\parallel$, as $v_\perp$ decreases. This simply means that the idealized situation of a straight line trajectory (with an abrupt cutoff in capture probability as a function of $v_\parallel$) is approached as $v_\perp \to 0$.

For the second system, p + W, even at $v = 0$ the discrete level is out of resonance with the much narrower conduction band of W (fig. 4b). Therefore, in general, the neutralization probability is smaller than for the Al surface (fig. 3b). At small $v_\parallel$, P_{B1} first increases with increasing $v_\perp$ corresponding to the requirement of higher perpendicular momentum components. At $v_\perp = 0.45$ kinematic resonance by the $v_\perp$-level shift occurs. Then, at still larger values of $v_\perp$, P_{B1} begins to decrease as in the previous example.

2.3. The second Born approximation

The IA capture amplitude in (6) or (8) describes a single scattering of a target electron off the projectile followed by an infinite-order scattering off the target represented by the cores of the lattice atom.s In principle then, this second scattering process involves a coherent sum of all possible sequences of scatterings $\{n_i\}$, where n_i denotes an n-times scattering process from the lattice cores labeled i. The totality of such scatterings is represented by the expansion of the operator $U_T V_T$ in (9), i.e.

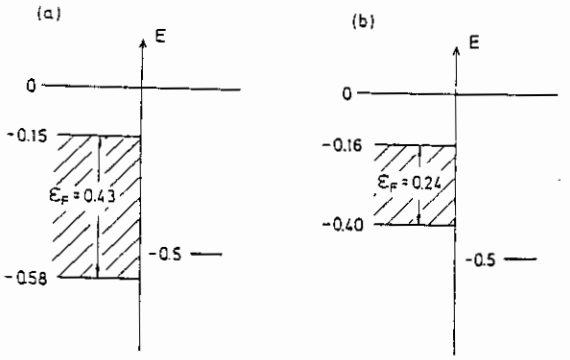

Fig. 4. (a) Energy level diagram for the aluminium conduction band and the ground state of hydrogen. (b) Same as (a) but for tungsten.

$$U_T(t, t')V_T = \exp\left\{-\mathrm{i}\left(K + \sum_i V_{ai}\right)(t - t')\right\} \sum_i V_{ai}, \tag{45}$$

where the sum over i is a sum over all lattice core potentials V_{ai} (considered identical). An approximation which has been much used in LEED theory (the kinematic approximation [22,24]), is to ignore contributions in (45) from scattering processes involving more than one lattice site at a time. Then the expansion in (45) reduces to

$$U_T(t, t')V_T \approx \sum_i \exp\{-\mathrm{i}(K + V_{ai})(t - t')\} V_{ai}. \tag{46}$$

With this approximation the corresponding incoming scattered electron wave in (9) is that arising from a coherent sum of scatterings at each lattice site taken separately.

Even with the simplification (46), the evaluation of the IA expression (8) is still a formidable task, since a 6-dimensional integral must be performed over momentum distributions in initial and final states. Since our aim here is to point out the major qualitative effects of scattering off the lattice cores, the further approximation will be made of treating this scattering in first order only, i.e. (45) is replaced by

$$U_T(t, t')V_T \approx U_0(t, t')V_T \equiv \exp\{-\mathrm{i}K(t, t')\} \sum_i V_{ai}. \tag{47}$$

This approximation represents a first Born approximation for the LEED-type lattice scattering and therefore

a second Born approximation for the overall electron capture amplitude. This second Born amplitude may be written as

$$f_{B2} = f_{B1} + f_2, \tag{48}$$

where f_{B1} is the first order amplitude discussed in section 2.1 and f_2 is the double scattering contribution

$$f_2 = \int_{-\infty}^{\infty} dt \int_t^{\infty} dt' \langle \Phi_f(t') | V_T U_0(t', t) V_P(t) | \Phi_i(t) \rangle. \tag{49}$$

Since

$$U_0(t', t) | q(t) \rangle = | q(t') \rangle, \tag{50}$$

introduction of a complete set of plane waves gives

$$f_2 = \int dq \int_{-\infty}^{\infty} dt \int_t^{\infty} dt' \langle \Phi_f(t') | V_T | q(t') \rangle \times \langle q(t) | V_P(t) | \Phi_i(t) \rangle. \tag{51}$$

Note that the scattering out of the initial state, by the projectile potential at time t, into the intermediate free state $|q(t)\rangle$ is separated in time from the subsequent scattering from this virtual state by the action of the target potential. Using the initial and final state momentum distributions and the broken straight line trajectory (11) and (12) as in section 2.1 allows f_2 to be written in the form,

$$\begin{aligned} f_2 = (2\pi)^{-3} \int dq\, dq'\, dp\, \tilde{V}_T(q' - q) \tilde{V}_P(q - p) \tilde{\phi}_i(p) \\ \times \exp\{i(p - q) \cdot b\} \\ \times \int_{-\infty}^{\infty} dt \exp\left\{ i(p - q) \cdot v(t) + i\left(\frac{q^2}{2} - \epsilon_i \right) t \right\} \\ \times \int_t^{\infty} dt' \tilde{\phi}_f^*(q' - v(t')) \\ \times \exp\{i(q' - v(t')) \cdot R(t')\} \\ \times \exp\left\{ i\left(\epsilon_f + \tfrac{1}{2}v^2 - \frac{q^2}{2} \right) t' \right\}. \end{aligned} \tag{52}$$

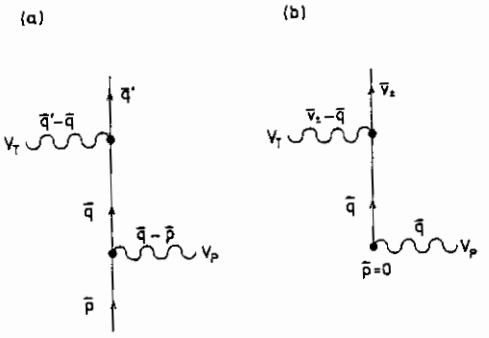

Fig. 5. Momentum diagram (laboratory frame) for the Thomas double scattering mechanism: (a) for capture of a jellium electron into a bound projectile state [compare eq. (54)]; (b) simplified process corresponding to an initial and final state peaking approximation.

The time integrals are performed by using the convergence factors $e^{-\eta|t|}$ and $e^{-\eta t'}$, $\eta \to 0^+$, appropriate to the prior form (1), (2) of the transition amplitude. Performing the time integrals, the above equation can then be expressed in a form analogous to (21) and (22)

$$f_2 = f_2^- + f_2^+, \tag{53}$$

with

$$\begin{aligned} f_2^{\pm} = \mp (2\pi)^{-3} \int dq\, dq'\, dp\, \tilde{\phi}_f^*(q' - v_{\pm}) \tilde{V}_T(q' - q) \\ \times \frac{1}{A^{\pm} + i\eta} \tilde{V}_P(q - p) \\ \times \tilde{\phi}_i(p) \exp\{i(q' + p - q - v_{\pm}) \cdot b\} \\ \times \left[\frac{-1}{B^- - i\eta} + \frac{1}{A^{\pm} + B^{\pm} \pm i\eta} \right], \end{aligned} \tag{54}$$

and

$$A^{\pm} \equiv q' \cdot v_{\pm} + \epsilon_f - \frac{v^2}{2} - \frac{q^2}{2}, \tag{55}$$

$$B^{\pm} \equiv (p - q) \cdot v_{\pm} + \frac{q^2}{2} - \epsilon_i. \tag{56}$$

Reading the integrand in (54) from right to left beginning with $\tilde{\phi}_i(p)$ the two scattering events are represented in momentum space by the diagrams shown in fig. 5 [27]. In fig. 5a the initial state is considered as a distribution of plane waves with momentum p. Each plane wave is scattered by the projectile with momentum transfer $q - p$ and strength $\tilde{V}_P(q - p)$ into a plane wave with momentum q. In the second scattering, this plane wave is scattered off the target with momentum transfer $q' - q$ and strength $\tilde{V}_T(q' - q)$ and results in a plane wave with momentum q'. The final state momentum distribution is peaked at $q' \approx v_{\pm}$.

In the high energy limit

$$|\epsilon_f| \ll \tfrac{1}{2}v^2, \qquad |\epsilon_f - \epsilon_i| \ll \tfrac{1}{2}v^2, \tag{57}$$

the classical Thomas scattering mechanism is recovered from (54) by investigating the poles of the propagators $[A^{\pm} + i\eta]^{-1}$ and of the factor $[A^{\pm} + B^{\pm} \pm i\eta]^{-1}$. For initial and final momentum distributions concentrated around $p \approx 0$ and $q' \approx v_{\pm}$, the propagator peaks at

$$A^{\pm} \approx 0 \qquad \text{or} \qquad q \approx v, \tag{58}$$

corresponding to an electron elastically scattered off the target (fig. 5b). The direction of q is determined by the peak of the second term in brackets in (54) at

$$A^{\pm} + B^{\pm} \approx 0 \qquad \text{or} \qquad q \cdot v_{\pm} \approx \tfrac{1}{2}v^2. \tag{59}$$

Finally, (58) combined with (59) implies an angle between q and $v_{\pm}$ of 60°. Hence, as in the collisions with gas targets [27], the peak structure in the integrand of (54) corresponds to the double-binary mechanism, illustrated in fig. 6. For a broken-line trajectory there are

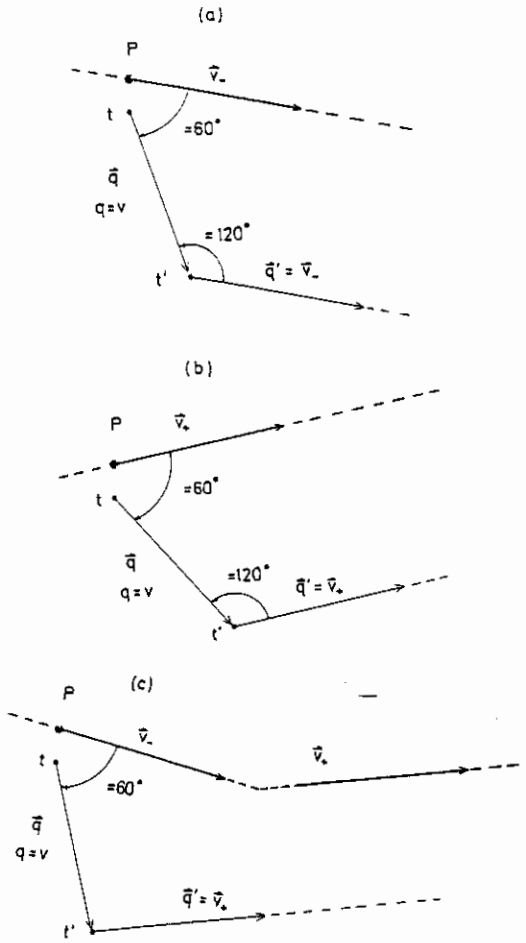

Fig. 6. Double-binary scattering mechanism in the second order process [see eq. (51)]. (a) The electron scatters off the projectile through an angle of 60° at time t. In the second binary collision the electron scatters off the target at time $t' > t$, again through an angle of 60°. Both collisions take place whilst the projectile is on the incoming trajectory (t, $t' < 0$). (b) As (a), but for the outgoing trajectory (t, $t' > 0$). (c) The scattering off the projectile happens at $t < 0$. The second scattering takes place at $t' > t$.

three distinct cases. In each case an initially stationary electron is scattered by the projectile at 60° to the projectile's direction, thereby acquiring the same speed as the projectile. In a subsequent elastic collision off the target lattice, the electron acquires the same velocity as the projectile. The small energy and momentum changes of the projectile during the first collision are neglected.

In the limiting case of a straight line trajectory, the first term contained in the brackets in (54) vanishes in the coherent sum of the incoming and outgoing path contributions (53). Analogously, in the second term the principal parts cancel giving

$$\frac{1}{A+B-\mathrm{i}\eta} - \frac{1}{A+B+\mathrm{i}\eta} = 2\pi\delta(A+B), \tag{60}$$

where the δ-function represents energy conservation, as explained for the corresponding first order expression (19). In this situation the three cases of Thomas scattering shown in fig. 6 become indistinguishable.

The evaluation of f_2^+ in the form (54) involves a 9-dimensional integral in momentum space. Nevertheless, the introduction of one additional approximation, appropriate to the capture into s-states at high velocity, allows this integral to be performed analytically. The approximation, much used in the theory of gas-phase collisions [5,26], is to replace $\boldsymbol{q}'$ in all terms in (54) except $A^{\pm}$ by its mean value $\boldsymbol{q}' \approx \boldsymbol{v}_{\pm}$. This replacement may not be made in the factor A since, in the limit $\frac{1}{2}v^2 \gg \Delta\epsilon$, this term (55) has a pole at $q = v$ when

$$\boldsymbol{q}' \approx \boldsymbol{v}^{\pm} \tag{61}$$

and therefore cannot be considered to be a slowly-varying function of $\boldsymbol{q}'$ around this value. Nevertheless, when this "peaking" approximation is made, the $\boldsymbol{q}'$ integral in (54) can be performed analytically and (54) is reduced to a six-dimensional integral,

$$f_2^{\pm} = \mp(2\pi)^{-3/2}\phi_{1s}(0)\int \mathrm{d}\boldsymbol{q}\,\mathrm{d}\boldsymbol{p}\,\tilde{V}_T(\boldsymbol{v}_{\pm}-\boldsymbol{q}) \times \frac{1}{A+\mathrm{i}Z_P v}\tilde{V}_P(\boldsymbol{q}-\boldsymbol{p})\tilde{\phi}_i(\boldsymbol{p}) \times \exp\{\mathrm{i}(\boldsymbol{p}-\boldsymbol{q})\cdot\boldsymbol{b}\}\left[\frac{-1}{B^- - \mathrm{i}\eta} + \frac{1}{A+B^{\pm}\pm\mathrm{i}\eta}\right], \tag{62}$$

with

$$A \equiv \epsilon_f + \tfrac{1}{2}(v^2 - q^2) \tag{63}$$

$$B^{\pm} \equiv (\boldsymbol{p}-\boldsymbol{q})\cdot\boldsymbol{v}_{\pm} + \frac{q^2}{2} - \epsilon_i. \tag{64}$$

We continue by specifying the target potential V_T. It is assumed to be periodic with respect to any plane parallel to the surface. Within a muffin tin model it is expressed as a sum over core or atomic potentials V_a centered around the lattice points ($\boldsymbol{R}_{\parallel,j}$, $\boldsymbol{R}_{\perp,l}$). Note that the top layer of ion cores is situated at half of a lattice constant inside the solid with respect to the electronic surface. Their position is given by $R_{\perp,0} = -d/2$, where d is the separation of layers parallel to the surface. The indices j and l count cores within a plane parallel to the surface and planes of lattice points parallel to the surface, respectively. For simplicity the core potential V_a is taken to be of the screened Coulomb type i.e.

$$V_a(r) = \frac{Z_T}{r}\exp\{-\lambda_T r\}. \tag{65}$$

For a first investigation we suppose a single cubic crystal of identical atoms. In this case $\boldsymbol{R}_{\parallel,j}$ can be

chosen as independent of the plane under consideration and the summation in (45) may be written explicitly as

$$V_T(r_\parallel, z) = \sum_l \sum_j V_a(r_\parallel - R_{\parallel,j}, z - R_{\perp,l}). \tag{66}$$

In momentum space the two dimensional periodicity of V_T is expressed by a two dimensional δ-function containing the parallel components of the momentum Q,

$$\tilde{V}_T(q) = \frac{(2\pi)^2}{A_{uc}} N \sum_l \exp\{-iQ_z R_{\perp,l}\} \times \sum_{g_\parallel} \delta^{(2)}(g_\parallel - Q_\parallel)\tilde{V}_a(Q), \tag{67}$$

such that only momenta with parallel component $q_\parallel$ equal to a reciprocal lattice vector $g_\parallel$ of the two dimensional surface-Bravais lattice can be transferred (Bragg condition). In the derivation of (67) the overlap between core potentials of neighboring muffin tins is neglected. The Fourier-transform of the core potential is $\tilde{V}_a$, N is the number of cores in a plane and A_{uc} is the area of the two dimensional unit cell.

With the initial states given by (29), the second order contribution (62) now becomes

$$f_2^{\pm} = \mp \frac{\sqrt{2\pi}}{A_{uc}} N \phi_{1s}(0) \sum_l \sum_{g_\parallel} \int dq_z\, dp_z \tilde{V}_a(g_\parallel, \pm v_\perp - q_z) \times \frac{1}{A + iZ_P v} \tilde{V}_P(v_\parallel - g_\parallel - k_\parallel, q_z - p_z)\tilde{u}_{k_z}(p_z) \times \exp\{i(p_z - q_z)b + i(q_z \mp v_\perp)R_{\perp,l}\} \times \left[\frac{-1}{B^- - i\eta} + \frac{1}{A + B^{\pm} \pm i\eta}\right], \tag{68}$$

where

$$A = \epsilon_f + \tfrac{1}{2}\left(v_\perp^2 + 2v_\parallel \cdot g_\parallel - g_\parallel^2 - q_z^2\right), \tag{69}$$

$$B^{\pm} = \left(k_\parallel - v_\parallel + g_\parallel\right)\cdot v_\parallel + \tfrac{1}{2}\left(v_\parallel - g_\parallel\right)^2 - \epsilon_i \pm (p_z - q_z)v_\perp + \frac{q_z^2}{2}. \tag{70}$$

The remaining two integrations in (68) have been performed analytically by two contour integrations (separately for the two cases $b > 0$ and $b < 0$, as subsequent to eq. (31)). In order to perform the q_z-integration, we slightly simplified the pole structure by dropping the q_z^2-term in the denominator of the first term in square brackets. This additional approximation is reasonable, since, for grazing incidence collisions, this term only provides a relatively small contribution to the coherent sum of $f_2^- + f_2^+$ (as mentioned above this term does not contribute at all for a straight line trajectory).

For large $v_\parallel$ ($v_\parallel \gg k_F$) the approximation

$$\left(k_\parallel - v_\parallel\right)\cdot g_\parallel \approx -v_\parallel \cdot g_\parallel \tag{71}$$

in the argument of $\tilde{V}_P$ is valid and the k-dependence of $f_2^{\pm}$ is contained in $k_\parallel'$ and k_z. The integration over the band momenta can then be performed as in (40) without further approximations.

The theory presented so far is still incomplete with respect to the specification of the three parameters N, Z_T, and λ_T.

According to (68) the second order contribution to the scattering amplitude is proportional to N, i.e. to the size of the surface. In the limit of an infinite surface it would lead to the prediction of an infinitely large amplitude. This problem arises since no account has yet been taken of the damping effect of the crystal on a beam of electrons propagating through it. In the theory of LEED this difficulty is circumvented by relating N to the number of cores within the part of the surface illuminated by the beam of incident electrons [22]. The origin of this N-dependence in our case is the assumption inherent in (52) that the whole crystal is bathed in plane waves with momenta q and q', where $|q\rangle$ is scattered into $|q'\rangle$ by the coherent action of N cores per plane. With respect to the number of planes and the number of scattering centres, N, in each plane, we now refer to the finite mean free path $\bar{\lambda}$ of electrons in solids. Electrons relevant to our calculation have a mean free path of roughly 5 Å [24]. As in the case of LEED we therefore only need to take into account a small number of layers, such that for most crystals only the surface layer and the next layer inside the solid are relevant. The sum over l in (66) is then restricted to two terms. An estimate of N is obtained by considering the number of cores contained in a circle of radius $\bar{\lambda}$ lying in the surface. For most metals this leads to $N \approx 5$ to 10.

With respect to the core potential (65) the screening of the (large) nuclear charge $Z_{T,nuc}$ by core and band electrons is taken into account by the parameters Z_T and λ_T. The screening constant, λ_T, represents screening of the central core charges by the metal electron gas. In the Thomas–Fermi approximation [29] it is given by

$$\lambda_T = \sqrt{\frac{3k_F}{\pi}}. \tag{72}$$

For tungsten ($k_F = 0.69$) it amounts to $\lambda_T = 0.81$ in fairly good agreement with the assumption inherent in the derivation of (67) of nonoverlapping core potentials: The inverse of λ_T is about one fourth of the lattice spacing, $d \approx 6$. As the effective core charge we use $Z_T = 1$, assuming complete screening by $Z_{T,nuc} - 1$ electrons. Since f_2 is directly proportional to both Z_T and N (and good estimates for both parameters are difficult to obtain), the product $Z_T N$ can be regarded, alternatively, as a parameter to be determined by comparison with experimental results.

We emphasize that the second Born contribution in distinction to the first Born, depends critically upon the properties of the crystal lattice. In view of the difficulty of assessing reliably these dependences, the results to be

presented below can be considered qualitative only. Indeed it is this qualitative aspect of higher-order scattering that we wish to emphasize. Nevertheless the major result of the paper is quantitative, namely, that above a collision velocity of approximately 3 a.u. (225 keV/amu) we would expect the contribution from the first Born process to be dominated by higher-order scattering off the lattice atoms. The second major conclusion of our study is that these higher- order contributions depend decisively upon whether the lattice cores act coherently or not in scattering the target electrons which are set in motion by an initial scattering off the projectile potential.

The qualitative nature of the second Born contribution is best illustrated by considering that a target electron of given initial momentum $\boldsymbol{k}$ is to be captured. Such an experiment could be performed in principle, although extremely difficult in practice. The effects of coherence on the nature of the double-scattering process is best seen by considering that initially only a single scattering centre (or an assembly of spatially uncorrelated centres) is present, as in the atomic case. For simplicity, a straight line trajectory $v_{\pm} = v$ parallel to the surface is assumed. The intermediate momentum $\boldsymbol{q}$ in (62) is to be integrated over and in the collision with the target a momentum $(v - \boldsymbol{q})$ is to transferred. The integral peaks near where the Thomas condition $q \approx v$, $\boldsymbol{q} \cdot \boldsymbol{v} \approx \frac{1}{2}v^2$ is satisfied. Since the potential V_T transfers momentum according to

$$\tilde{V}_T(\boldsymbol{q} - \boldsymbol{v}) \sim \left[|\boldsymbol{v} - \boldsymbol{q}|^2 + \lambda_T^2 \right]^{-1} \tag{73}$$

or

$$\tilde{V}_T(\boldsymbol{q} - \boldsymbol{v}) \sim \left[q^2 + \lambda_T^2 \right]^{-1} \tag{74}$$

at the Thomas peak, independent of v, the Thomas condition can be satisfied for all incident velocities v. The singularity in q for each value of v is integrable and provides a smoothly decreasing capture probability $P(b)$ as v increases.

However, in the case of a periodic target potential V_T as in (66), the Fourier transform (67) contains an additional δ-function. The straight line trajectory provides also the δ-function (60). Then the amplitude (62) contains the factor (in the light energy limit)

$$\begin{aligned} &\delta(g_y + q_y)\delta(g_x - v + q_x)\delta\left(q_x v - \tfrac{1}{2}v^2\right) \\ &\quad = \delta(g_y + q_y)\delta\left(g_x - \tfrac{1}{2}v\right)\delta\left(q_x v - \tfrac{1}{2}v^2\right). \end{aligned} \tag{75}$$

Then one sees that since $\tilde{V}_T$ can only transmit given values of momenta parallel to the surface, the second Born scattering can lead to capture only for distinct values of the incident velocity, given by

$$v = 2g_x, \tag{76}$$

where g_x is the component of a reciprocal lattice vector parallel to v, i.e. parallel to the surface. We remind

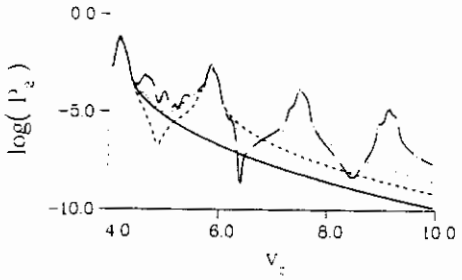

Fig. 7. Second-order contribution to the differential K-shell capture probability dP_2/dk with $k = (0.5, 0.1, 0.5)$ in the collision of a proton with an aluminium surface. The different curves are for ——— $n_{max} = 2$; - - - - - - $= 3$; ····· $= 4$; -·-·-· $= 5$.

ourselves that under the same assumptions, i.e. high velocity and straight line motion, the first Born approximation is identically zero for all v.

For not necessarily very high velocities, the generalization of (76) is

$$v = k_x + g_x + \sqrt{(k_x + g_x)^2 + 2(\epsilon_t + V_0) - k^2}, \tag{77}$$

which again follows from (60).

As with the first Born, the effect of the broken-line trajectory and the momentum distribution of initial and final states serves to smear out these effects and gives a finite capture probability for all velocities. Nevertheless, peaks remain, localized near velocities given by (76) as seen in fig. 7. This figure also illustrates the extreme dependence of the high-$v_{\parallel}$ capture probability on the reciprocal lattice structure. There are n_{max} peaks in the probability according as the sum in (68) is over reciprocal lattice vectors

$$\boldsymbol{g}_{\parallel} = (g_x, g_y) = \frac{2\pi}{d}(n_x, n_y), \tag{78}$$

with

$$n_{x,y} = -n_{max}, \ldots, n_{max}. \tag{79}$$

For a given n_{max} there are $(2n_{max} + 1)^2$ reciprocal lattice vectors in the sum.

The total probability of electron capture from the the second-order process alone is given by (cf. eq. (39)),

$$P_2 = \int_{k \le k_F} \mathrm{d}\boldsymbol{k}\ \rho\, |f_2(\boldsymbol{k})|^2. \tag{80}$$

When capture only from a given state of momentum $\boldsymbol{k}$ in the band is considered we compute the differential probability

$$\frac{\mathrm{d}P_2}{\mathrm{d}\boldsymbol{k}} = \rho\, |f_2(\boldsymbol{k})|^2. \tag{81}$$

In fig. 7, this quantity is shown for a square surface lattice with lattice spacing $d = 7.7$ a.u., appropriate for an aluminium surface. Only the surface layer is taken

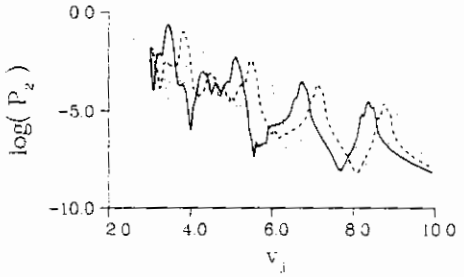

Fig. 8. As fig. 7 with $n_{max} = 5$, but $k = (k_x, 0.1, 0.5)$, where —— $k_x = 0.1$; - - - - - - $= 0.3$; · · · · · · $= 0.5$.

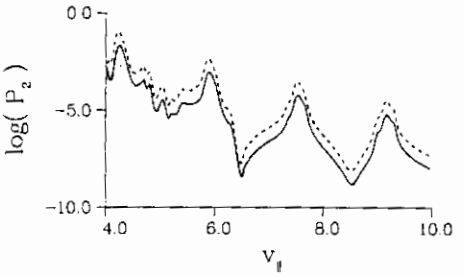

Fig. 9. As fig. 8 but for $k = (0.5, 0.1, k_z)$ with —— $k_z = 0.1$; - - - - - - $= 0.3$.

into account and a perpendicular velocity of 0.1 a.u. is assumed.

In the exact evaluation of (62), the nature of the peaks in the second-order capture probability is dependent upon the jellium momentum k. There are two effects. The peaks in dP_2/dk shift their position according to the x-component of k, as shown in fig. 8 (cf. eq. (77)). They remain nearly fixed in position but change their magnitude as k_z increases as shown in fig. 9. This latter effect is consistent with an increasing transmission coefficient with increasing k_z, so that for fixed impact parameter more electron density is encountered. Both fig. 8 and fig. 9 are for an aluminium surface.

The shift of the peak has the consequence that an integral over k smooths out the structure. Hence the total capture probability, calculated from eq. (80) and shown in fig. 10 for an aluminium surface, is relatively smooth, although some vestiges of the structure do remain. Most importantly, however, fig. 10 shows that at the high velocities considered here the second-order capture probability is roughly two orders of magnitude larger than the first-order. The capture probability in fig. 10, integrated over the contributions of all occupied band states at zero temperature is for $v_\perp = 0.1$, $n_{max} = 2$, $N = 5$ and $\lambda_T = 0.94$. The distance of closest approach b has been calculated within the Lindhard continuous string model [30], in connection with a Thomas–Fermi interatomic potential. This yields a distance of closest approach to the top layer of 0.13 a.u., or $b = -3.72$. The projectile nucleus therefore penetrates deeply into the electronic surface. All features of figs. 7 to 10 when calculated for a tungsten surface are qualitatively the same as for an aluminium surface. In the former case however, the dominance of the second-order contribution over the first-order is more pronounced than in fig. 10, since the first-order contribution diminishes more rapidly with $v_\parallel$, due to the fact that the unperturbed proton 1s level is out of resonance with the band states.

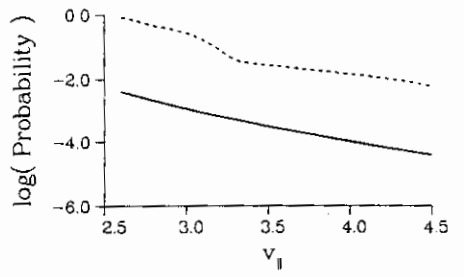

Fig. 10. First-order P_{B1} and second-order P_2 contribution to the K-shell capture probability. —— P_{B1}; - - - - - - P_2.

3. Conclusions

We have considered the role of the double scattering process in the capture of electrons from surfaces by ions at grazing incidence. In this mechanism electrons are not captured directly (a three body collision) but are first scattered by the incident ion to acquire a speed equal to that of the ion. They then scatter elastically off the solid (a process similar to LEED) to emerge from the surface with a velocity similar to that of the ion, thereby facilitating their capture. For quasi-free band electrons we have shown that this double-scattering mechanism is the dominant mode of capture when the ion velocity component parallel to the surface greatly exceeds the electron Fermi velocity. We remark also that this mechanism should give important contributions to the momentum distribution of free electrons ejected from the surface by fast, grazing incidence ion beams.

We would like to thank J. Burgdörfer for several valuable comments. One of us, U.T., thanks the University of Tennessee in Knoxville and Oak Ridge National Laboratory for hospitality whilst this work was in progress.

References

[1] Dž, Belkić, R. Gayet and A. Salin, Phys. Rep. 56 (1979) 279.

[2] R. Shakeshaft and L. Spruch, Rev. Mod. Phys. 51 (1979) 369.
[3] J.S. Briggs in: Semiclassical Description of Atomic and Nuclear Collisions, eds. J. Bang and J. de Boer (Elsevier, Amsterdam, 1985) p. 183.
[4] L.H. Thomas, Proc. R. Soc. (London) A114 (1927) 561.
[5] K. Dettmann and G. Leibfried, Z. Phys. 218 (1969) 1.
[6] J.S. Briggs, P.T. Greenland and L. Kocbach, J. Phys. B15 (1982) 3085.
[7] L. Kocbach and J.S. Briggs, J. Phys. B17 (1984) 3255.
[8] M.R.C. McDowell, Proc. R. Soc. (London) A264 (1961) 277.
[9] I.M. Cheshire, Proc. R. Soc. (London) 84 (1964) 89.
[10] Dž. Belkić and R. Gayet, J. Phys. B10 (1977) 1911.
[11] J.S. Briggs, J. Phys. B10 (1977) 3075.
[12] J. Macek and S. Alston, Phys. Rev. A26 (1982) 250.
[13] K. Taulbjerg and J.S. Briggs, J. Phys. B16 (1983) 3811.
[14] H.J. Andrà, R. Zimny, H. Winter and H. Hagedorn, Nucl. Instr. and Meth. B9 (1985) 572.
[15] H.J. Andrä, in: Fundamental Processes of Atomic Dynamics, NATO ASI Series vol. B181, eds. J.S. Briggs, H. Kleinpoppen and H.O. Lutz (Plenum, 1988).
[16] H. Winter, Nucl. Instr. and Meth. B2 (1984) 286.
[17] K.J. Snowdon, R. Hentschke, A. Närmann and W. Heiland, Nucl. Instr. and Meth. B23 (1987) 309.
[18] S.S. Shekter, Zh. Eksp. Teor. Fiz. 7 (1937) 750.
[19] J.W. Gadzuk, Surf. Sci. 6 (1967) 133.
[20] B.A. Trubnikov and Y.N. Yavlinskii, Sov. Phys.-JETP25 (1967) 1089.
[21] J. Burgdörfer, E. Kupfer and H. Gabriel, Phys. Rev. A35 (1987) 4963.
[22] J.B. Pendry, Low Energy Electron Diffraction (Academic Press, London, 1974).
[23] K. Heinz, Appl. Phys. A41 (1986) 3.
[24] M.A. van Hove, W.H. Weinberg and C.-M. Chan, Low Energy Electron Diffraction, Springer Series in Surface Science (Springer, Berlin, 1986).
[25] K. Dettmann, in: Springer Tracts in Modern Physics, vol. 58 (Springer, Berlin, 1971).
[26] J.S. Briggs and L. Dubé, J. Phys. B13 (1980) 771.
[27] L.S. Dubé and J.S. Briggs, J. Phys. B14 (1981) 4595.
[28] R.M. May, Phys. Rev. 136 (1964) A669.
[29] C. Kittel, Introduction to Solid State Physics, 3rd ed. (Wiley, New York, 1966) p. 237.
[30] J. Lindhard, K. Dan. Vidensk. Selsk. Mat. Fys. Medd. 34 (1965) no. 4.